Electronic structure of heavily doped graphene: The role of foreign atom states

Matteo Calandra and Francesco Mauri

CNRS and Institut de Minéralogie et de Physique des Milieux Condensés, Case 115, 4 Place Jussieu, 75252, Paris Cedex 05, France
(Received 31 August 2007; published 30 October 2007; corrected 31 October 2007)

Using density functional theory calculations we investigate the electronic structure of graphene doped by deposition of foreign atoms. We demonstrate that, as the charge transfer to the graphene layer increases, the band structure of the pristine graphene sheet is substantially affected. This is particularly relevant when Ca atoms are deposed on graphene at CaC_6 stoichiometry. Similarly to what happens in superconducting graphite intercalated compounds, a Ca band occurs at the Fermi level. Its hybridization with the C states generates a strong nonlinearity in one of the π^* bands below the Fermi level, at energies comparable to the graphene E_{2g} phonon frequency. This strong nonlinearity, and not many-body effects as previously proposed, explains the large and anisotropic values of the apparent electron-phonon coupling measured in angular resolved photoemission.

The discovery of superconductivity in CaC_6 (Refs. [1–3]) demonstrates that superconducting critical temperatures (T_c's) as large as 15 K can be obtained in graphite intercalated compounds (GICs). The recent availability of graphene monolayer[4,5] and the possibility of deposing foreign atoms on top, considerably widens the number of GICs. Indeed the constraints for deposition onto graphene are milder than those required for graphite intercalation. Consequently even larger T_c's could be discovered in these systems.

At low dopings, K deposition on graphene, angular resolved photoemission (ARPES) measurements,[6–9] and first principles calculations[10–13] have shown that (i) the graphene band-structure below ϵ_f is weakly affected by the presence of K atoms and (ii) a marked kink occurs at 0.195 eV below ϵ_f, an energy corresponding to the E_{2g} graphene phonon frequency.

At high doping, a very promising result for high T_c superconductivity is the report of a massive enhancement of the electron-phonon coupling in graphene doped by Ca atoms deposition[14] as measured in ARPES. In Ref. [14] stoichiometry as large as CaC_6 was achieved. The ARPES measured electron-phonon coupling has been shown to be very anisotropic with values ranging from 0.5 to 2.3, suggesting that a heavily doped graphene monolayer could be superconducting with large critical temperatures and large anisotropic superconducting gap(s). Such large and anisotropic values of the electron-phonon coupling were interpreted as due to many-body effects and to the occurrence of a Van Hove singularity. The ARPES measurement of the electron-phonon coupling is indirect since it relies on the renormalization of the Fermi velocity by the interaction. However, such a renormalization could be ascribed to other mechanisms such as nonlinearity in the bare bands or interaction with other quasiparticles. To validate the claim of a huge electron-phonon coupling in heavily doped graphene a complete characterization of the electronic structure is mandatory.

In this work we use density functional theory calculations to interpret the huge and highly anisotropic electron-phonon coupling observed in heavily doped graphene by ARPES in terms of the CaC_6 monolayer band structure.

In ARPES the spectral weight is measured, namely, for a given band index,

$$A(\mathbf{k},\epsilon) = \frac{-2[\Sigma''_{\mathrm{all}}(\mathbf{k},\epsilon)]}{[\epsilon - \epsilon_\mathbf{k} - \Sigma'_{\mathrm{all}}(\mathbf{k},\epsilon)]^2 + [\Sigma''_{\mathrm{all}}(\mathbf{k},\epsilon)]^2}, \qquad (1)$$

where $\Sigma'_{\mathrm{all}}(\mathbf{k},\epsilon)$ and $\Sigma''_{\mathrm{all}}(\mathbf{k},\epsilon)$ are the real and imaginary parts of the electron self-energy $\Sigma_{\mathrm{all}}(\mathbf{k},\epsilon)$, and $\epsilon_\mathbf{k}$ are the single particle bands. The total electron self-energy includes contributions from all the interactions in the system. The electron-phonon coupling parameter is

$$\lambda_\mathbf{k} = - \left. \frac{\partial \Sigma'(\mathbf{k},\epsilon)}{\partial \epsilon} \right|_{\epsilon=\epsilon_f}, \qquad (2)$$

where $\Sigma(\mathbf{k},\epsilon)$ is the electron-phonon contribution to the electron self-energy and $\Sigma'(\mathbf{k},\epsilon)$ its real part. In what follows we assume that the dominant contribution to the electron self-energy is given by the electron-phonon coupling, $\Sigma_{\mathrm{all}}(\mathbf{k},\epsilon) \approx \Sigma(\mathbf{k},\epsilon)$.

The maximum position in the spectral weight is given by the relation $\epsilon_\mathbf{k}^{\mathrm{max}} - \epsilon_\mathbf{k} - \Sigma'(\mathbf{k},\epsilon_\mathbf{k}^{\mathrm{max}}) = 0$. Linearizing $\Sigma'(\mathbf{k},\epsilon) \approx -\lambda_\mathbf{k}\epsilon$ leads to $\lambda_\mathbf{k} = \frac{\epsilon_\mathbf{k}}{\epsilon_\mathbf{k}^{\mathrm{max}}} - 1$. If the bare bands behave linearly, namely $\epsilon_k = \hbar v_0 k$, and if the renormalized can be linearized at ϵ_f, $\epsilon_\mathbf{k}^{\mathrm{max}} = \hbar v_f k$,[11,15] then $\lambda_\mathbf{k}$ and

$$\lambda_\mathbf{k} = \frac{v_0}{v_f} - 1, \qquad (3)$$

where v_f is obtained from a linear fit to the maximum position in momentum distribution curves (MDCs) at energies close to ϵ_f, while v_0 is obtained from a linear fit in an appropriate energy window below the kink where the bare bands are linear. Note that if the bare bands are not linear then Eq. (3) is incorrect.

In experiments a finite resolution affects substantially the energy window close to ϵ_f so that the determination of v_f is nontrivial. The the following quantity is then computed:

$$\lambda_{\mathrm{ARPES}} = \frac{v_0}{v_{\mathrm{ARPES}}} - 1, \qquad (4)$$

where now v_{ARPES} is obtained from a linear fit to the maximum position in MDCs in an energy window ranging from

the kink energy up to the Fermi level. Clearly $\lambda_{ARPES} \approx \lambda$ only if $v_f \approx v_{ARPES}$. Consequently the energy window chosen to fit v_{ARPES} is crucial. This has been demonstrated to be important in graphene at low electron-doping.[11] Indeed, in the case of rigid band doping of the graphene π^* bands, where the electron-phonon coupling can be calculated analytically,[10,11] it has been found that $\lambda_{ARPES} \approx 2.5\lambda$. Thus in this case, λ_{ARPES} cannot provide a quantitative information of the electron-phonon coupling since v_{ARPES} depends critically on the fit procedure.

So far, the electronic structure of atoms deposed on graphene has been interpreted in terms of the pristine graphene band structure.[6–9] This is correct if the charge transfer to the graphene layer (doping) is weak as in the K-deposition on graphene. However, this is questionable for larger dopings, since foreign atom states could affect the band structure below the Fermi level (ϵ_f). Indeed in GICs, an intercalant band crosses ϵ_f.[10,17,18] Thus in the case of a CaC$_6$ monolayer the electronic structure at ϵ_f could be substantially affected by the Ca states. For this reason we calculate the single particle band structure of monolayer and bulk CaC$_6$ using density functional theory (DFT). We assume that the Ca deposition leads to an ordered $\sqrt{3} \times \sqrt{3}$ structure with axes rotated of 30° with respect to the standard C$_2$ crystal structure. Simulating a single layer requires very large cells to converge due to the finite electric dipole formed by the Ca donor and the graphene acceptor. The problem can be solved using a double slab geometry with two specular layers of CaC$_6$ separated by vacuum along the z direction. This geometry has zero net electric dipole. The interstitial space between Ca atoms on different layers is 11 Å while that between the two graphene layers is 10 Å. We optimize the in-plane graphene lattice parameter (a) and the distance (z) between the Ca atoms and the nearby graphene layer, obtaining a=2.47 Å and z=2.315 Å. Note that in bulk CaC$_6$ structural optimization leads to a=2.50 Å and z=2.60 Å.[18] Electronic structure calculations are performed using the ESPRESSO code[19] and the generalized gradient approximation.[20] We expand the wave functions and the charge density using 35 and 600 Ry cutoffs, respectively. The electronic integration for the double slab geometry has been performed using a $8 \times 8 \times 8$ k-points mesh and a Gaussian smearing of 0.05 Ry. For graphene we use a $30 \times 30 \times 2$ k-points mesh.

In Fig. 1 we show the band structure of a CaC$_6$ monolayer compared to that of graphene using the same in-plane lattice parameter, a=2.47 Å. The energies of the Dirac point in the two structures have been aligned. In the CaC$_6$ monolayer Brillouin zone the Dirac point is refolded at Γ due to the $\sqrt{3} \times \sqrt{3}R30°$ surface deposition. Because of this superstructure, a small gap opens at the Dirac point in the CaC$_6$ monolayer. The Fermi level is crossed by two carbon π^* bands and a third band mainly Ca in character. The steepest π^* band (labeled π_1^*) is very similar to that of C$_2$, while the other π^* (labeled π_2^*) is substantially affected by the Ca recovering. The most striking feature is, however, the occurrence of an additional band at ϵ_f, having dominant Ca character. This band is the so-called "intercalant" band in GICs,[10,17] descending to lower energies with respect to its position in CaC$_6$ bulk. The bottom of the intercalant band is at −1.15 eV
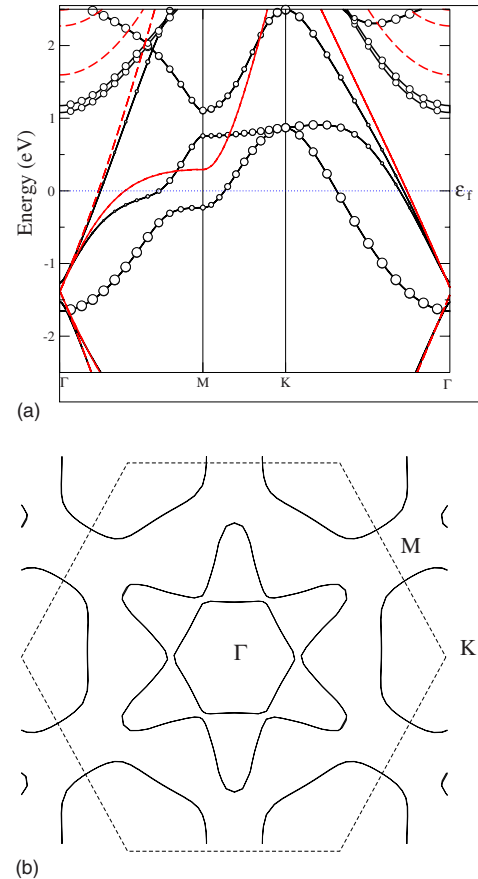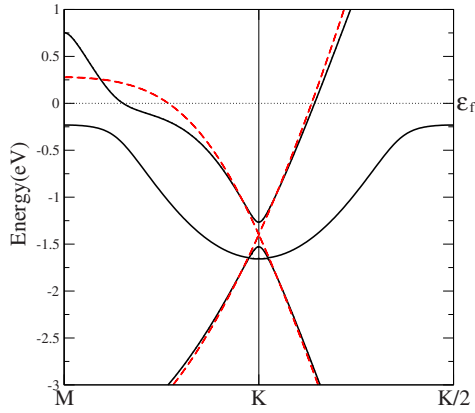

FIG. 1. (Color online) (a) Band structure of CaC$_6$ monolayer (black continuous line) and graphene (red continuous and dashed) using the same in-plane lattice parameter, namely a=2.47 Å. The size of the circles indicates the percentage of Ca character (see Ref. 10) in a given band. (b) Fermi surface of CaC$_6$ monolayer. The special points labels refer to the CaC$_6$ hexagonal Brillouin zone.

with respect to ϵ_f in bulk CaC$_6$ and is now at −1.65 eV in the monolayer. Correspondingly the graphene Dirac point is at $\approx$−2.04 eV in the bulk and at $\approx$1.39 in the monolayer, in nice agreement with experiments.[14] This effect is well-known; in alkaline-earths GICs, the intercalant band descends as the interlayer distance is reduced.[17,18,16]

Finally, in the CaC$_6$ monolayer there is a marked avoided crossing between the π_2^* band and the Ca band along ΓM. In this direction, approaching the M point, there is a large hybridization between the two bands, as it is evident from the change in the Ca character of the band. Most important, a large deviation from linearity occurs in the π_2^* band at an energy of $\approx$0.2 eV below the Fermi energy. This energy is very close to the E_{2g} phonon frequency[21] of undoped graphene at the Γ point, namely $\omega_{E_{2g}\Gamma}$=0.195 eV.

The Fermi surface of the CaC$_6$ monolayer is shown in Fig. 1(b) in the CaC$_6$ monolayer Brillouin zone and in Fig. 2(b) in the C$_2$ Brillouin zone. In Fig. 1(b) the Fermi surface is composed of a 6-points star centered at Γ formed by the intersection of two triangular shapes. In addition there are six hole pockets centered around **K** and **K′**. The hexagon within the star is due to the π_1^* band, while the outer perimeter of the star is composed by the π_2^* band hybridized with Ca

(a)
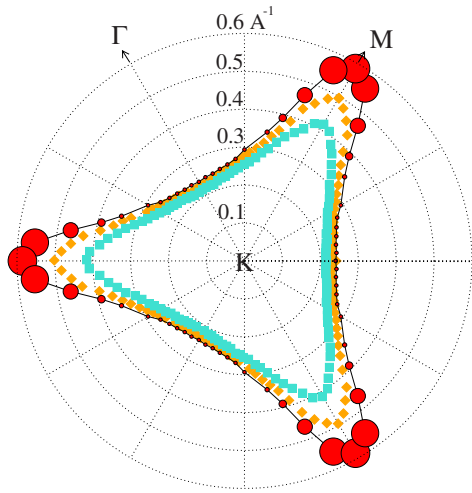
(b)
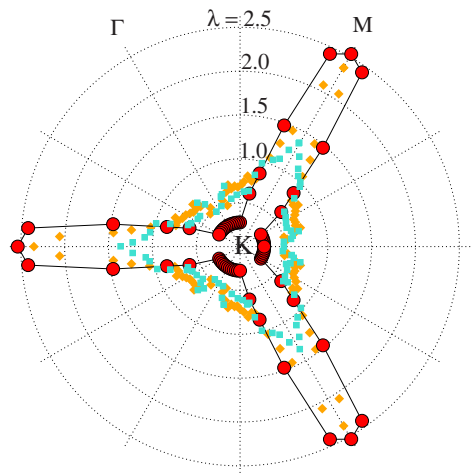
(c)

FIG. 2. (Color online) (a) Band structure of CaC_6 monolayer (black continuous) and of graphene (red dashed) plotted in the graphene Brillouin zone. (b) Fermi surface of CaC_6 as a function of doping. Square and diamonds are data from Ref. 14 and refer to the dopings labeled Ca (top) and Ca (under) K 2×2 (top). Circles are theoretical calculations. The size of the circles is proportional to λ_{ARPES}. (c) Polar plot of λ_{ARPES}. The high-symmetry points are labeled with respect to the C_2 Brillouin zone.

states. Along ΓK the star has dominant C character, while along ΓM it has strongly hybridized Ca and C character. The hole pockets are mostly Ca. In Fig. 2(b) one of the triangular shapes composing the star is compared with the Fermi surface determined by ARPES.[14] A very good agreement is found for the surface at the highest experimental doping.

In Fig. 2, the CaC_6 monolayer and C_2 bands are plotted in the C_2 Brillouin zone. The aforementioned deviation from linearity in the π_2^* bands, now occurring along **MK**, results in an apparent kink. However, this kink is not due to the electron-phonon interaction or to many-body effects, but it is due to the nonlinearity of the single particle bands. The change in slope is induced indirectly by the hybridization with the intercalant band.

In order to compare with experimental data, we estimate the "apparent" electron-phonon coupling λ_{ARPES} [Eq. (4)] generated by the change in slope of the single particle band. We obtain v_0 and v_{ARPES} in Eq. (3) by linear fits to the π_2^* band at several directions departing from the **K** point in the C_2 Brillouin zone. The fits to obtain v_{ARPES} and v_0 are performed in the energy range -0.2 eV $< \epsilon - \epsilon_f < 0$ eV and -1.0 eV $< \epsilon - \epsilon_f < -0.2$ eV, respectively. A strong anisotropy in λ_{ARPES} is obtained as a result of the single-particle band structure. Values as large as 2.5 are found along the **KM** direction. Along ΓK, where no kink is present in the bare bands, a zero value is found.

To compare with experiments the contribution due to the electron-phonon coupling in the CaC_6 monolayer should be added. In ARPES spectra in Ref. 14 the only visible contribution is that due to the in-plane graphene phonons at ≈ 0.2 eV. In bulk CaC_6 this contribution is 0.11.[10] As we have shown in Ref. 11, the fitting procedure used in Ref. 14 overestimates λ by a factor of 2.5. Thus to the anisotropic bare band contribution we added an isotropic electron-phonon contribution of 0.275.

The results are illustrated as polar plots in Figs. 2(b) and 2(c) and are compared to the experimental data of Ref. 14 in Fig. 2(c). We reproduce the strong anisotropy observed in ARPES experiment[14] and the huge values of λ_{ARPES} along the **KM** direction. In the **K**Γ direction, where the bare band contribution is zero, the value of λ_{ARPES} is given entirely by the electron-phonon contribution. In this direction the values of λ for bulk CaC_6 underestimate the experimental one. This could be due to a larger density of states at the Fermi level in the CaC_6 monolayer with respect to bulk CaC_6. Indeed we found that the monolayer density of states at the Fermi level is 1.7 times larger than that in the bulk.

In this Rapid Communication we have studied the electronic structure of foreign atoms deposed on graphene. We have shown that as the charge transfer to graphene becomes significant, the band structure cannot anymore be interpreted in terms of the pristine graphene π^* bands. When Ca is deposed on graphene at stoichiometry comparable with CaC_6, a Ca band occurs at the Fermi level. This band is the surface analog of the intercalant band in superconducting graphite intercalated compounds[10,17] that is crucial to understand the superconducting behavior of these compounds. The Ca bands strongly hybridize with the C π^* states and induces a marked nonlinearity in one of the π^* bands at energies comparable to $\epsilon_f - \omega_{E_{2g}} \Gamma$. This nonlinearity explains the large and strongly

anisotropic values of λ_{ARPES} in the CaC_6 monolayer. However, as shown in this work, these large and anisotropic values do not provide any information on the real electron-phonon coupling in the system.

[1] T. E. Weller, M. Ellerby, S. S. Saxena, R. P. Smith, and N. T. Skipper, Nat. Phys. **1**, 39 (2005).

[2] N. Emery, C. Hérold, M. d'Astuto, V. Garcia, Ch. Bellin, J. F. Marêché, P. Lagrange, and G. Loupias, Phys. Rev. Lett. **95**, 087003 (2005).

[3] A. Gauzzi, S. Takashima, N. Takeshita, C. Terakura, H. Takagi, N. Emery, C. Herold, P. Lagrange, and G. Loupias, Phys. Rev. Lett. **98**, 067002 (2007).

[4] K. S. Novoselov and A. K. Geim, Nat. Mater. **6**, 183 (2007.

[5] C. Berger *et al.*, J. Phys. Chem. B **108**, 19912 (2004).

[6] K. S. Novoselov, A. K. Geim, S. V. Morozov, D. Jiang, M. I. Katsnelson, I. V. Gregorieva, S. V. Dubonos, and A. A. Firsov, Nature (London) **438**, 197 (2005).

[7] S. Y. Zhou, G.-H. Gweon, C. D. Spataru, J. Graf, D.-H. Lee, Steven G. Louie, and A. Lanzara, Phys. Rev. B **71**, 161403(R) (2005).

[8] S. Y. Zhou, G.-H. Gweon, J. Graf, A. V. Fedorov, C. D. Spataru, R. D. Diehl, Y. Kopelevich, D.-H. Lee, Steven G. Louie, and A. Lanzara, Nat. Phys. **2**, 595 (2006).

[9] A. Bostwick, T. Ohta, T. Seyller, K. Horn, and E. Rotenberg, Nat. Phys. **3**, 36 (2007).

[10] M. Calandra and F. Mauri, Phys. Rev. Lett. **95**, 237002 (2005).

[11] M. Calandra and F. Mauri, arXiv:0707.1467, Phys. Rev. B (to be published).

[12] Wang-Kong Tse and S. Das Sarma, arXiv:0707.3651 (unpublished).

[13] Cheol-Hwan Park, Feliciano Giustino, Marvin L. Cohen, and Steven G. Louie, Phys. Rev. Lett. **99**, 086804 (2007).

[14] J. L. McChesney, A. Bostwick, T. Ohta, K. V. Emtsev, T. Seyller, K. Horn, and E. Rotenberg, arXiv:0705.3264 (unpublished).

[15] G. Grimvall, *The Electron-Phonon Interaction in Metals* (North-Holland, Amsterdam, 1981), p. 201.

[16] Lilia Boeri, Giovanni B. Bachelet, Matteo Giantomassi, and Ole K. Andersen, Phys. Rev. B **76**, 064510 (2007).

[17] G. Csányi, P. B. Littlewood, A. H. Nevidomskyy, C. J. Pickard, and B. D. Simons, Nat. Phys. **1**, 42 (2005).

[18] M. Calandra and F. Mauri Phys. Rev. B **74**, 094507 (2006).

[19] http://www.pwscf.org; S. Baroni *et al.*, Rev. Mod. Phys. **73**, 515 (2001).

[20] J. P. Perdew, K. Burke, and M. Ernzerhof, Phys. Rev. Lett. **77**, 3865 (1996).

[21] M. Lazzeri and F. Mauri, Phys. Rev. Lett. **97**, 266407 (2006).